Published in final edited form as:
Proc IEEE Int Symp Biomed Imaging. 2009 June 28; 2009: 831–834. doi:10.1109/ISBI.2009.5193181.

A DATA-DRIVEN APPROACH TO PRIOR EXTRACTION FOR SEGMENTATION OF LEFT VENTRICLE IN CARDIAC MR IMAGES

Xiao Jia,
Department of Electrical & Computer Engineering, National University of Singapore, Singapore 117576, Singapore

Chao Li,
Department of Electrical & Computer Engineering, National University of Singapore, Singapore 117576, Singapore

Ying Sun,
Department of Electrical & Computer Engineering, National University of Singapore, Singapore 117576, Singapore

Ashraf A. Kassim,
Department of Electrical & Computer Engineering, National University of Singapore, Singapore 117576, Singapore

Yijen L. Wu,
Pittsburgh NMR Center for Biomedical Research, Carnegie Mellon University, Pittsburgh, PA 15213, USA

T. Kevin Hitchens, and
Pittsburgh NMR Center for Biomedical Research, Carnegie Mellon University, Pittsburgh, PA 15213, USA

Chien Ho
Pittsburgh NMR Center for Biomedical Research, Carnegie Mellon University, Pittsburgh, PA 15213, USA

Abstract

In this paper, we propose a data-driven approach that extracts prior information for segmentation of the left ventricle in cardiac MR images of transplanted rat hearts. In our approach, probabilistic priors are generated from prominent features, i.e., corner points and scale-invariant edges, for both endo- and epi-cardium segmentation. We adopt a level set formulation that integrates probabilistic priors with intensity, texture, and edge information for segmentation. Our experimental results show that with minimal user input, representative priors are correctly extracted from the data itself, and the proposed method is effective and robust for segmentation of the left ventricle myocardium even in images with very low contrast. More importantly, it avoids inter- and intra- observer variations and makes accurate quantitative analysis of low-quality cardiac MR images possible.

Index Terms

cardiac MRI; segmentation; left ventricle; prior leaning

1. INTRODUCTION

Cardiac Magnetic Resonance Imaging (MRI) has been increasingly used as a noninvasive tool in small animal studies of heart diseases and transplant rejections [1,2]. Reliable quantitative

analysis of cardiac MRI requires accurate segmentation of the left ventricle (LV) which is tedious and time-consuming when performed manually. Although many methods have been proposed for automatic segmentation of human hearts, few methods have been reported for small animal hearts. The STACS method proposed in [3] has been shown to produce relatively accurate segmentation results on shortaxis cardiac MR images of a rat, by combining region-based and edge-based information with an elliptical shape prior and contour smoothness constraint.

In this paper, we focus on short-axis cardiac MR images of transplanted rat hearts in a study for non-invasive early detection of acute cardiac allograft rejection [4]. Such images are extremely difficult to segment due to their low spatial resolution, low signal-to-noise ratio (SNR), and lack of contrast at the myocardial boundaries. Moreover, turbulent blood flow often causes confusing edges in the LV cavity. To overcome these difficulties, it is important to incorporate into the segmentation framework all available prior knowledge about the anatomical structures to be segmented.

For integration of prior knowledge, most existing segmentation methods use shape priors. In [3] and [5], elliptical shape priors were used for both endo- and epi-cardium by including a shape prior term in the energy functional. Learned from training samples, probabilistic shape priors proposed in [6] constrain the segmentation process by optimizing a statistical metric between the evolving contour and the prior model. However, in addition to the disadvantage of requiring manually processed training samples, such shape priors may not be able to provide a good shape representation for a particular image. For these reasons, it is desirable to extract priors from the data itself without the training process, and the priors therefore are representative for that particular image.

This paper describes a semi-automated segmentation method that integrates automatically derived priors with region-based (i.e., intensity and texture) and edge-based information into a level set framework. For each image, we first detect prominent feature points (i.e., corner points and scale-invariant edges) and compute their corresponding confidence measures. Statistical priors are generated using mostly high confidence points; and these priors are then incorporated into the level set framework through prior probability maps. By including high confidence priors as strong constraints into the segmentation process, the proposed method is able to segment the LV of transplanted rat hearts with good accuracy.

The rest of the paper is organized as follows. Section 2 describes in detail our proposed method. The experimental results are discussed in Section 3, followed by the conclusion in Section 4.

2. METHODOLOGY

Our proposed method consists of three main steps: 1) preprocessing to enhance contrast and remove inhomogeneity; 2) automatic extraction of probabilistic priors from prominent features; and 3) level set formulation that incorporates the extracted priors to constrain the segmentation.

2.1. Preprocessing

For each slice, a rough center of the epicardium is provided by the user to correctly initialize the region of interest (ROI), according to which the images are cropped.

Due to low contrast and inhomogeneity of raw cardiac MR images of transplanted rat hearts, preprocessing including contrast enhancement as well as inhomogeneity correction are performed prior to feature extraction. Image contrast is enhanced by histogram equalization, and inhomogeneity is corrected by the algorithm proposed by Axel et al. in [7]. As shown in

Fig. 1(c), after pre-processing, edges in the original MR images are enhanced, while systematic intensity inhomogeneity is removed.

2.2. Probabilistic prior learning

Level set evolution without prior knowledge cannot provide accurate segmentation and may result in leaking due to noise and complexity of organ structures. To overcome this problem, probabilistic priors are automatically generated based on extracted features. Prominent feature points, i.e. corner points and scale-invariant edges, are detected respectively as good indicators of the LV cavity and the epicardium. To remove undesired feature points, we assume that the point provided by user is close to the true center of epicardium and the shape of the epicardium is approximately circular.

Prior for endocardium segmentation—Compared to blob detectors, corner detectors are more robust against intensity inhomogeneities inside the LV cavity region caused by turbulent blood flow. Here we use the algorithm proposed by Rosten and Drummond in [8,9] to detect corner points. These corner points are mostly located either inside the LV cavity or outside the epicardium, with very few in the myocardium. Therefore, it is possible to filter out corner points outside the LV cavity. Taking the center point provided by the user as the origin, we convert all corner points to polar coordinates and obtain the distribution of the corner points with respect to radius R. A threshold radius R^* is then calculated using Gaussian mixture models to extract the corner points inside the LV cavity (see Fig. 2(a)).

Using the extracted corner points as sample points, for the LV cavity, a relative probability density function having values in the range [0, 1], $p_{\text{prior}}(x, y)$, is obtained by kernel density estimation. To avoid the domination of priors in the energy functional, we define a conservative prior probability map as:

$$P_{\text{prior}}(x,y)=\begin{cases} p_{\text{prior}}(x,y) & \text{if } p_{\text{prior}}(x,y)>0.5 \\ 0.5 & \text{otherwise} \end{cases}. \quad (1)$$

As shown in Fig. 2(b), a high prior probability indicates that the point is more likely to be inside the LV cavity than outside. On the other hand, a prior probability of 0.5 indicates no preference between the inside and outside of the LV cavity.

Prior for epicardium segmentation—We extract priors for epicardial contour based on the scale-invariant edges detected by the method described in [10,11]. In order to select edges along the epicardium, we firstly filter out undesired ones by examining edge directions: desired edges should be tangent to the epicardium, which is approximately circular. If a detected edge and the corresponding radial direction are nearly perpendicular, the edge is preserved; otherwise, the edge is discarded.

In polar coordinates, we remove edges inside the LV cavity using the threshold R^* obtained previously. After that, edges along the epicardium can be approximately extracted by selecting edges with radius in the range from $\tilde{R}$ to $\tilde{R} + \Delta r$, where $\tilde{R}$ is the minimum radius value of edges not inside the cavity and Δr is a tolerance distance that assures the true boundary is inside its capture range. In our experiments, Δr is set to be 10 pixels.

Let $S_{i,j}$ denote the set of extracted edges in the jth frame of the ith slice. Since the epicardium is generally approximately circular, we estimate the distribution of edge points along radial directions. Let $N(\mu_{i,\theta}, \sigma^2_{i,\theta})$ denote a global Gaussian distribution of the epicardial radius, estimated from edge points from all frames of ith slice along angle θ and its neighboring

directions. To estimate the distribution $N(\mu_{ij,\theta}, \sigma^2_{ij,\theta})$ for the jth frame, we first remove outliers from set $S_{i,j}$ based on $N(\mu_{i,\theta}, \sigma^2_{i,\theta})$. Next, we estimate the distribution of the epicardial radius in different directions using the remaining edge points. In case the edge points are not detected along certain directions in the jth frame, we use the global distribution $N(\mu_{i,\theta}, \sigma^2_{i,\theta})$ to approximate $N(\mu_{ij,\theta}, \sigma^2_{ij,\theta})$. By mapping the estimated distributions $N(\mu_{ij,\theta}, \sigma^2_{ij,\theta})$ back to Cartesian coordinates, the probabilistic map (normalized to [0, 1]) of the epicardium for a particular frame, as the one shown in Fig. 2(d), can be obtained.

2.3. Level set formulation

Once the priors are successfully extracted, we integrate them with intensity, texture and edge information into a level set formulation to guide the contour evolution. For texture feature extraction, we adopt the same approach as in [12] using structure tensor and nonlinear diffusion.

For a contour C, which is embedded as the zero level set of function φ, the energy functional is defined as:

$$J(\varphi)=\lambda_r J_r(\varphi)+\lambda_e J_e(\varphi), \tag{2}$$

where $J_r(\varphi)$ is the region-based term incorporating extracted priors and image features, i.e., intensity and texture; $J_e(\varphi)$ is the edge-based term moving the contour towards the object boundaries; and λ_r and λ_e are weights that regulate relative strength of the region-based and edge-based terms. In our experiments, we set $\lambda_r = 1$ and $\lambda_e = 0.5$ for both endo- and epi-cardium segmentation.

The edge-based term $J_e(\varphi)$ is common for both endo- and epi-cardium segmentation. Let g be an inverse edge indicator function:

$$g=\frac{1}{1+|\nabla G_\sigma * I|^2}, \tag{3}$$

where G_σ is the Gaussian kernel with standard deviation σ and I is the preprocessed image. Thus, J_e is given by

$$J_e(\varphi)=\int_\Omega g\delta_\varepsilon(\varphi(x,y))|\nabla\varphi(x,y)|dxdy, \tag{4}$$

where δ_ε is the regularized Dirac function.

Endocardium segmentation—The region-based term $J_r(\varphi)$ for endocardium segmentation is defined as the combination of intensity, texture and the prior probabilities extracted from corner points using (1).

Following the same notation as in [12], we construct a vector-valued image $u = (u_1, \ldots, u_4)$. The probability density functions for vector $u(x, y)$ to be in the foreground Ω_1 and the background Ω_2 can be estimated by

$$p_i(u(x,y))=\prod_{k=1}^{4} p_{k,i}(u_k(x,y)) \quad i \in \{1,2\}, \tag{5}$$

where $p_{k,i}$ ($u_k(x, y)$) represents the likelihood of $u_k(x, y)$ belonging to Ω_i, based on the kth channel (I, I_x^2, I_y^2 or I_xI_y) of the feature space specified in [12]. The region-based term is then defined as

$$J_r(\varphi)=-\int_{\Omega_1} \ln\left[p_1(u(x,y))\cdot P_{\text{prior}}(x,y)\right] dxdy-\int_{\Omega_2} \ln\left[p_2(u(x,y))\cdot(1-P_{\text{prior}}(x,y))\right] dxdy, \tag{6}$$

where $P_{\text{prior}}(x, y)$ is the probabilistic map for the LV cavity shown in Fig 2(b). Finally, the level set evolution equation can be derived as:

$$\frac{d\varphi}{dt}=\delta_\varepsilon(\varphi)\left[\lambda_r \ln\frac{p_1(u)\cdot P_{\text{proir}}}{p_2(u)\cdot(1-P_{\text{prior}})}+\lambda_e \text{div}\left(g\frac{\nabla\varphi}{|\nabla\varphi|}\right)\right]. \tag{7}$$

Epicardium segmentation—We initialize the epicardial contour using the edge distributions $N(\mu_{ij,\theta}, \sigma_{ij,\theta}^2)$ obtained in Section 2.2. For each angle θ, point with radius $\mu_{ij,\theta}$ is chosen to be on the initial contour.

To avoid over-segmentation, logic operations [13] are performed on different feature channels to obtain the prior probability map for epicardium segmentation. As shown in Fig. 1(h), the combination of likelihood ratio maps from all feature channels using logic operations provide a conservative and good representation of the epicardium.

Unlike the segmentation of the endocardium, the region-based term in epicardium segmentation incorporates the extracted priors by applying a spatially varying weight $\omega(x, y) = 1 - P_{\text{prior}}(x, y)$, where $P_{\text{prior}}(x, y)$ is the probabilistic map shown in Fig. 2(d). Therefore, the level set evolution equation is defined as follows:

$$\frac{d\varphi}{dt}=\delta_\varepsilon(\varphi)\left[\lambda_r\omega \ln\frac{p_1(u)}{p_2(u)}+\lambda_e \text{div}\left(g\frac{\nabla\varphi}{|\nabla\varphi|}\right)\right], \tag{8}$$

where p_1 and p_2 are probability density maps for points belong to Ω_1 and Ω_2, respectively. These two maps are obtained by combining all feature channels using logic operations.

As a result, the spatially varying weight ω constrains contour evolution such that: for regions in which the epicardial boundary has been detected with high confidence, the contour evolves according to the force derived from the edge-based term only; whereas for locations at which the epicardial boundary is not detected or detected with very low confidence, the contour is driven by a combined force stemming from both region-based and edge-based terms.

3. RESULTS

We tested the proposed method on 2 slices of short-axis cardiac MR images (10 images per slice), which had been manually segmented by an expert. These 256 by 256 images come from

two transplanted rat studies and were acquired by a Brucker AVANCE DRX 4.7 tesla system at the Pittsburgh NMR Center for Biomedical Research in Pittsburgh, PA, USA.

In Fig. 3 we compare the segmentation results obtained by our proposed method and by manual segmentation. The endocardial and epicardial boundaries detected by our proposed method are very close to their manual counterparts. Moreover, the resulting myocardial contours are generally visually more consistent with the neighboring frames than the manually drawn ones.

To quantitatively evaluate the segmentation results, we measure the area similarity, S_{area}, between the myocardium mask detected by our method and the corresponding mask by manual segmentation. For the 20 images tested in our experiments, S_{area} has a mean value of 0.86 with standard deviation 0.03. This suggests that our results are comparable to those have been reported in [3], in which images with better quality were used. Here S_{area} is defined as:

$$S_{\text{area}} = \frac{2n(A_1 \wedge A_2)}{n(A_1)+n(A_2)}, \tag{9}$$

where A_1 and A_2 are binary images whose "on" pixels represent the regions of the segmented object, Λ is the element-wise "and" operator, and $n(A)$ represents the cardinality of A or the number of "on" pixels in the binary image A.

Regarding user interaction, the proposed method only requires the user to provide one point per slice, while the rest process is completely automatic. The average running time is about 3 minutes per slice (containing 10 images) in a MATLAB environment on a workstation with 3.0 GHz quad core CPU. The running time can be greatly reduced if our method was implemented in a more efficient programming language such as C++.

4. CONCLUSION

In this paper, we propose a data driven prior extraction approach to segment the myocardium of the LV in cardiac MR images. Our proposed method is able to automatically extract priors for endo- and epi-cardium segmentation from corner points and scale-invariant edges, respectively. The extracted priors are incorporated in a level set formulation to constrain the segmentation. Unlike existing segmentation methods based on priors, our approach avoids the training process and it generates more representative priors for a particular image. Preliminary experiments on short-axis cardiac MR images with low contrast and low SNR have shown promising results, both qualitatively and quantitatively. In the future we plan to carry out more detailed validation.

Acknowledgments

This work was supported by NUS grant R-263-000-470-112.

We thank Dr. Kazuya Sato for performing transplant surgeries on rats.

References

1. Stuckey DJ, Carr CA, Tyler DJ, Aasum E, Clarke K. A novel MRI method to detect altered left ventricular ejection and filling patterns in rodent models of disease. Magnetic Resonance in Medicine Aug;2008 60:582–587. [PubMed: 18727095]
2. Wu YJL, Sato K, Ye Q, Ho C. MRI investigations of graft rejection following organ transplantation using rodent models. Methods Enzymol 2004;386:73–105. [PubMed: 15120247]

3. Pluempitiwiriyawej C, Moura JMF, Wu Y-JL, Ho C. STACS: New active contour scheme for cardiac MR image segmentation. IEEE Trans Med Imag May;2005 24(5):593–603.

4. Wu, Y-JL.; Sato, K.; Sun, Y.; Chang, H.; Hitchens, K.; Moura, JMF.; Ho, C. Non-invasive early detection of acute cardiac allograft rejection by MRI in rodent model. Proc. ISMRM 12th Annual Meeting; May 2004; p. 15-21.

5. Chen T, Babb J, Kellman P, Axel L, Kim D. Semi-automated segmentation of myocardial contours for fast strain analysis in cine displacement-encoded MRI. IEEE Trans Med Imag Aug;2008 27:1084–1094.

6. Rousson M, Paragios N. Prior knowledge, level set representations and visual grouping. International Journal of Computer Vision Jul;2007 76(3):231–243.

7. Axel L, Costantini J, Listerud J. Intensity correction in surface coil MR imaging. American Journal of Radiology Feb;1987 148(2):418–420.

8. Rosten, E.; Drummond, T. Fusing points and lines for high performance tracking. Proc. ICCV; Nov 2005; p. 1508-1515.

9. Rosten, E.; Drummond, T. Machine learning for high-speed corner detection. Proc. ECCV; May 2006; p. 430-443.

10. Kokkinos, I.; Maragos, P.; Yuille, A. Bottom-up and top-down object detection using primal sketch features and graphical models. Proc. CVPR; Jun 2006; p. 1893-1900.

11. Kokkinos, I.; Yuille, A. Unsupervised learning of object deformation models. Proc. ICCV; Oct 2007; p. 1-8.

12. Rousson, M.; Brox, T.; Deriche, R. Active unsupervised texture segmentation on a diffusion based feature space. Proc. CVPR; Jun 2003; p. 699-704.

13. Sandberg B, Chan T. Logic operators for active contours on multi-channel images. J Vis Commun Image R 2005;16:333–358.

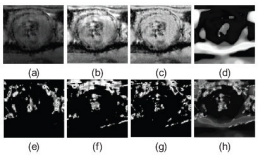

Fig. 1.

Preprocessing results and extracted feature channels: (a) cropped original image; (b) after contrast enhancement; (c) after inhomogeneity correction; (d)–(g) likelihood ratio maps for feature channels I, I_x^2, I_y^2 and I_x,I_y, respectively; and (h) combination of (d)–(g) using logic operations.

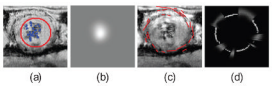

Fig. 2.
Extraction of priors: (a) selected corner points; (b) prior probability map for endocardium segmentation; (c) selected edges on a single frame; (d) prior probability map for epicardium segmentation.

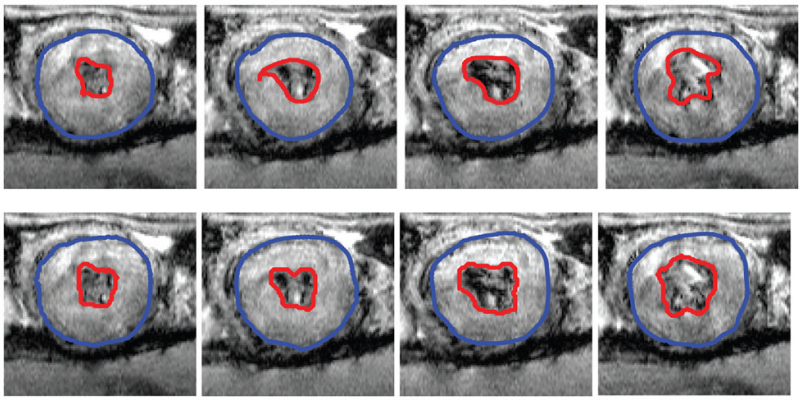

Fig. 3.
Comparison of segmentation results by manual segmentation (first row) and our proposed method (second row).